ADVANCED SCIENCE
Open Access

Supporting Information

for *Adv. Sci.*, DOI 10.1002/advs.202303057

Advanced Soft Porous Organic Crystal with Multiple Gas-Induced Single-Crystal-to-Single-Crystal Transformations for Highly Selective Separation of Propylene and Propane

Lin Li, Shuhong Zhao, Huiming Huang, Muyao Dong, Jie Liang, Hui Li, Jian Hao, Engui Zhao and Xinggui Gu**

Supporting Information

Advanced Soft Porous Organic Crystal with Multiple Gas-Induced Single-Crystal-to-Single-Crystal Transformations for Highly Selective Separation of Propylene and Propane

Lin Li, Shuhong Zhao, Huiming Huang, Muyao Dong, Jie Liang, Hui Li, Jian Hao, Engui Zhao, and Xinggui Gu**

Experimental procedures

Materials and instruments

Single-crystal X-ray diffraction (SCXRD) data were collected on a Gemini E X-ray diffractometer (Agilent, Oxford) with graphite-monochromator Mo-Kα (λ = 0.71073 Å) at about 110 K. Powder X-ray diffraction (PXRD) patterns were collected on a Bruker X-ray diffractometer (D8 ADVANCE X) using Cu-Kα radiation. The gas adsorption isotherms were collected on an automatic volumetric adsorption apparatus of BSD-PS (M) (Specific surface area & pore size analyzer). The breakthrough experiments were carried out in a dynamic gas breakthrough of BSD-MAB (Multi-component Adsorption Breakthrough Curve Analyzer). Differential scanning calorimetry (DSC) characterizations were conducted on a NETZSCH DSC214 instrument.

Preparation of SPOC-SQ-a microcrystalline powder

The microcrystalline powder of SPOC-SQ-DCM was obtained by slow evaporation in a saturated DCM solution of SPOC-SQ, and then activated in air under room temperature for at least 6 h, generating the SPOC-SQ-a microcrystalline powder.

Single-component gas adsorption of SPOC-SQ-a microcrystalline for C1, C2, and C3 hydrocarbons

The gas adsorption isotherms were collected on an automatic volumetric adsorption apparatus BSD-PS (M) (Specific surface area & pore size analyzer). Before the adsorption measurements, the as-prepared sample (SPOC-SQ-a) was dried under high vacuum for 24 h at 60 °C for gas adsorption analyses. The different temperatures for gas adsorption measurements were maintained by using ice salt bath, ice bath, and water bath. After gas adsorption measurements were completed, the sample was evacuated by a vacuum pump for 6 h at 60 °C until the pressure was below 0.1 bar to ensure complete removal of adsorbent.

Gate-opening enthalpy

The Clausius-Clapeyron equation was used to calculate the molar enthalpy of gate opening (ΔH_{GO}).

$d\ln P_{GO}/(d(1/T)) = \Delta H_{GO}/R$

P_{GO} is gate opening pressure, T is measurement temperature, R is gas constant (8.314 J mol^{-1} K^{-1}).

Preparation of SPOC-SQ-a single crystal

The single crystal of SPOC-SQ-a was easily obtained by slow removal of DCM from SPOC-SQ-DCM single crystal in air at room temperature.

Preparation of SPOC-SQ-CO_2 and SPOC-SQ-CO_2-MO single crystals

Single crystal of SPOC-SQ-CO_2 was obtained by placing SPOC-SQ-a single crystal in CO_2 gas atmosphere at about 1 bar under 203 K (acetone and liquid nitrogen) for about 12 h. SPOC-SQ-CO_2 single crystal could be transformed to SPOC-SQ-CO_2-MO single crystal upon vacuum treatment at room temperature for 1 h, which could be further activated back to SPOC-SQ-a by vacuuming at 60 °C for 3 h.

Preparation of SPOC-SQ-C_2H_2 and SPOC-SQ-C_2H_2-MO single crystals

Single crystal of SPOC-SQ-C_2H_2 was obtained by placing SPOC-SQ-a single crystal in C_2H_2 gas atmosphere at about 1 bar under 298 K for about 12 h. SPOC-SQ-C_2H_2 single crystal could be transformed to SPOC-SQ-C_2H_2-MO single crystal upon vacuum treatment at room temperature for more than 30 min, which could be further activated back to SPOC-SQ-a by vacuuming at 60 °C for 3 h.

Preparation of SPOC-SQ-C_2H_4, SPOC-SQ-C_2H_4-MO, and SPOC-SQ-C_2H_4-MSO single crystals

Single crystal of SPOC-SQ-C_2H_4 was obtained by placing SPOC-SQ-a single crystal in C_2H_4 gas atmosphere at about 1 bar under 253 K (ice salt bath: 500 g crushed ice and 164.89 g sodium chloride) for about 12 h. SPOC-SQ-C_2H_4 single crystal could be transformed to SPOC-SQ-C_2H_4-MO and SPOC-SQ-C_2H_4-MSO single crystals upon treatment in air at room temperature for about 5 and 60 min, respectively, which could be further activated back to SPOC-SQ-a by vacuuming at 60 °C for 3 h.

Preparation of SPOC-SQ-C_2H_6, SPOC-SQ-C_2H_6-MO, and SPOC-SQ-C_2H_6-MSO single crystals

Single crystal of SPOC-SQ-C_2H_6 was obtained by placing SPOC-SQ-a single crystal in C_2H_6 gas atmosphere at about 1 bar under 253 K (ice salt bath: 500 g crushed ice and 164.89 g sodium chloride) for about 12 h. SPOC-SQ-C_2H_6 single crystal could be transformed to SPOC-SQ-C_2H_6-MO and SPOC-SQ-C_2H_6-MSO single crystals upon treatment in air at room temperature for about 20 s and 30 min, respectively, which could be further activated back to SPOC-SQ-a in air for more than 3 h.

Preparation of SPOC-SQ-C_3H_4 single crystal

Single crystal of SPOC-SQ-C_3H_4 was obtained by placing SPOC-SQ-a single crystal in C_3H_4 gas atmosphere at about 1 bar under 273 K for about 12 h. SPOC-SQ-C_3H_4 single crystal could be activated back to SPOC-SQ-a by vacuuming at 60 °C for 3 h.

Preparation of SPOC-SQ-C_3H_6 and SPOC-SQ-C_3H_6-MO single crystals

Single crystal of SPOC-SQ-C_3H_6 was obtained by placing SPOC-SQ-a single crystal in C_3H_6 gas atmosphere at about 1 bar under 273 K for about 12 h. SPOC-SQ-C_3H_6 singe crystal could be transformed to SPOC-SQ-C_2H_4-MO single crystals upon treatment in air at room temperature for about 40 s, which could be further activated back to SPOC-SQ-a in air for more than 30 min.

Single crystal X-ray crystallographic resolution

The structures were solved by the direct method and refined by the full-matrix least-squares method on F^2 with anisotropic thermal parameters for all non-hydrogen atoms. Gas molecules of CO_2, C_2H_2, C_2H_4, C_2H_6, C_3H_4, and C_3H_6 were located from enough electron density peaks

and refined with isotropic displacement parameters. Due to the gas molecular movements inside the SPOC-SQ frameworks, the crystallographic analysis was carried out through reasonable refinements to ensure their positions, the resolved results met the normal bond lengths (1.174 Å of C-O for CO_2, 1.136 Å, 1.298 Å, and 1.591 Å for C-C in C_2H_2, C_2H_4, and C_2H_6, respectively, 1.174 Å and 1.466 Å for C-C in C_3H_4, and 1.309 Å and 1.514 Å for C-C in C_3H_6). Hydrogen atoms on C_2H_2, C_2H_4, C_2H_6, C_3H_4, and C_3H_6 molecules were added with geometrical constraints. Crystallographic data and structure refinement data were shown in Tables S2-S7. Further supplementary crystallographic data for the above single crystals can be obtained free of charge from the Cambridge Crystallographic Data Centre via www.ccdc.cam.ac.uk/data_request/cif (CCDC number: 2220252-2220269).

Computational methods

The first-principles calculations were carried out within the framework of density functional theory (DFT) within the general gradient approximation (GGA) by Perdew-Burke-Ernzerhof (PBE) exchange-correlation functional using the QUICKSTEP module in the CP2K package.[1] Double-zeta valence plus polarization (DZVP) basis sets was employed, combined through norm-conserving Goedecker-Teter-Hutter (GTH) pseudo potentials[2-3] and the Gaussian and Augmented Plane Wave (GAPW) hybrid basis set.[4] The DFTD3 correction[5] was included in the calculation to fully capture the long-range dispersion interaction between the framework of SPOC-SQ-gas and gas molecules. The crystal and adsorption structures were fully relaxed until the maximum atomic force was less than 2×10^{-2} eV $Å^{-1}$.

PXRD analysis of microcrystalline powders

PXRD patterns were collected by a Bruker X-ray diffractometer using Cu-Kα radiation. The data were collected in the range of 2θ = 5° - 45°. In-situ PXRD patterns were collected at different time after placing SPOC-SQ-gas in air for 12 hours. (Gases: CO_2 and C_2H_2)

DSC for SPOC-SQ-CO_2-MO and SPOC-SQ-C_2H_2-MO crystals

DSC analyses were conducted on a NETZSCH DSC214 instrument. Single crystals of SPOC-SQ-CO_2-MO and SPOC-SQ-C_2H_2-MO obtained after removal of CO_2 and C_2H_2 from SPOC-SQ-CO_2 and SPOC-SQ-C_2H_2 were placed in Tzero aluminum pans and heated from 273 K to the 373 K at a rate of 5, 10, or15 K min^{-1}.

Single-component gas adsorptions for MSME of SPOC-SQ-CO_2-MO and SPOC-SQ-C_2H_2-MO

The gas adsorption isotherms were collected on an automatic volumetric adsorption apparatus BSD-PS (M) (Specific surface area & pore size analyzer). Before the adsorption measurements, the as-synthesized sample (SPOC-SQ-DCM) was dried under high vacuum for 24 h at 60 °C to remove the DCM molecules, giving the activated SPOC-SQ-a for gas adsorption analyses. Gas adsorption tests for CO_2 and C_2H_2 were maintained at 253 K and 298 K by using ice salt bath and water bath, respectively. The second to fifth cycle of absorption tests were performed without activation.

Isotherm data were analyzed using the virial equation

$$\ln(n/P) = A_0+A_1n+A_2n^2+\cdots$$

where P is pressure, n is the amount adsorbed, and A_0, A_1, A_2, etc., are virial coefficients. A_0 is related to adsorbate-adsorbent interactions, whereas A_1 describes adsorbate-adsorbate interactions. The Henry's law constant (K_H) is equal to exp (A_0), and the selectivity can be obtained from K_H.

Breakthrough separation experiments for C_3H_6/C_3H_8 (*v*/*v*, 50/50) separation

In a typical two-gas breakthrough experiment, 4.2 g of pre-activated, tandem-packed sample was placed in quartz tubing (10 mm diameter) to form a fixed bed. The adsorbent bed was purged under a 60 cm^3/min flow of He gas at 60 °C for 2 h before the breakthrough experiment. Upon cooling to 0 °C, a 5 cm^3/min gas mixture containing 50% C_3H_6 and 50% C_3H_8 was introduced. The outlet composition was continuously monitored by BSD-MS until a complete

breakthrough was achieved. When the outlet composition of two gases reached equilibrium, gas mixture flow was then shut off.

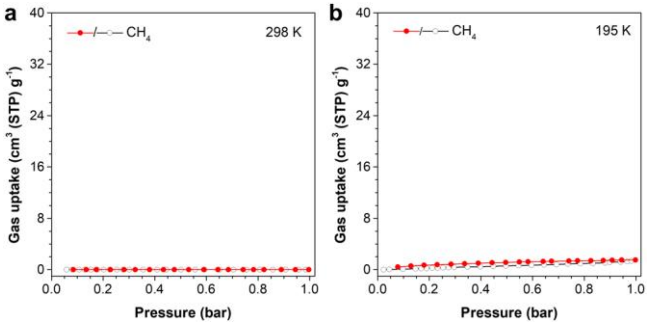

Figure S1. Sorption isotherms of SPOC-SQ-a towards CH_4 at (a) 298 K and (b) 195 K. Filled and open circle symbols represent adsorption and desorption, respectively.

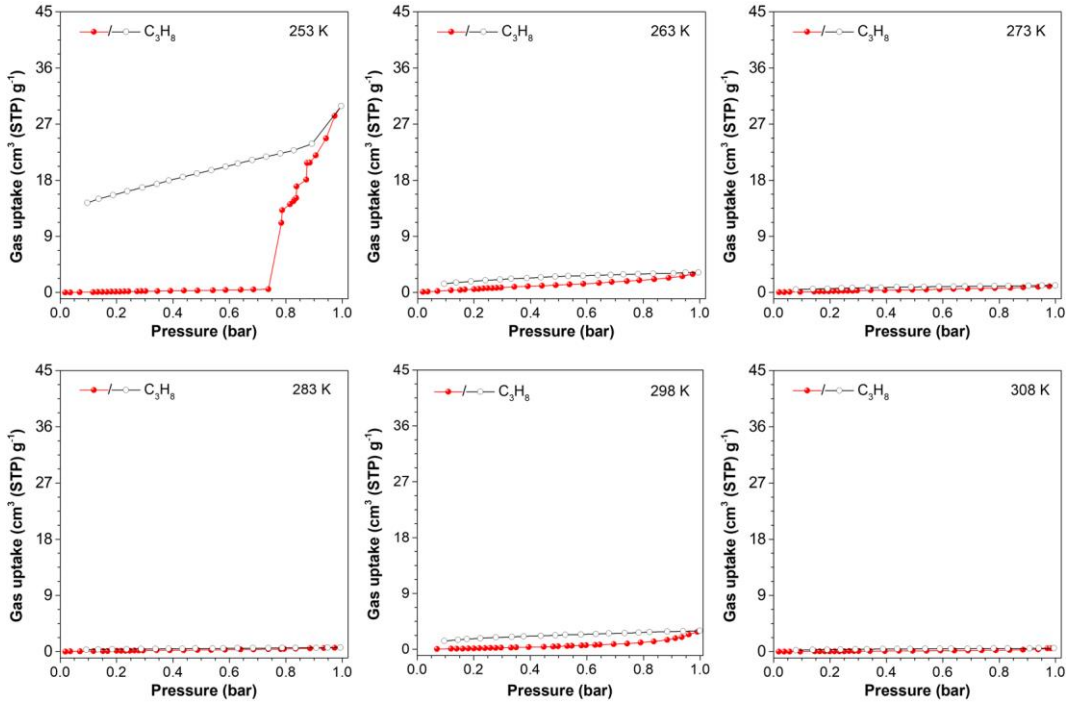

Figure S2. Sorption isotherms of SPOC-SQ-a towards C_3H_8 at 253 K, 263 K, 273 K, 283 K, 298 K, and 308 K. Filled and open circle symbols represent adsorption and desorption, respectively.

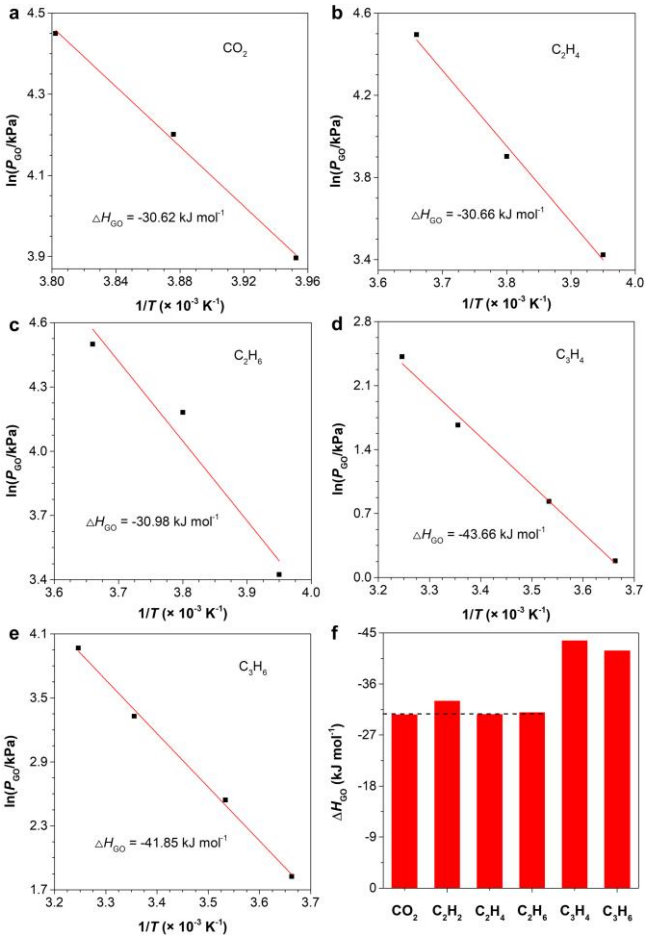

Figure S3. Plots of gate-opening pressure ($\ln P_{GO}$) vs inverse of measurement temperature ($1/T$) for adsorption isotherms of (a) CO_2, (b) C_2H_4, (c) C_2H_6, (d) C_3H_4, and (e) C_3H_6. (f) Comparison of their enthalpies of gate opening (ΔH_{GO}) obtained according to the Clausius-Clapeyron equation: $d\ln P_{GO}/(d(1/T)) = \Delta H_{GO}/R$.

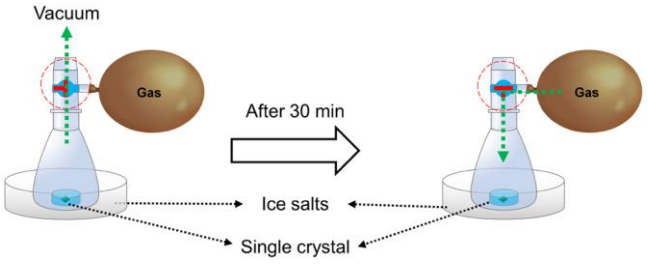

Figure S4. Schematic illustration of the apparatus used for the single crystal growth in gas atmosphere at low temperature.

Table S1. Single crystal growth conditions under gas atmosphere.

Gas	**CO_2**	**C_2H_2**	**C_2H_4**	**C_2H_6**	**C_3H_4**	**C_3H_6**

Temperature (K)	203	298	253	253	273	273
Pressure (bar)	1	1	1	1	1	1

Table S2. Crystal data and structure refinement of SPOC-SQ-CO_2, SPOC-SQ-CO_2-MO, and SPOC-SQ-a after CO_2 removal.

Name	SPOC-SQ-CO_2	SPOC-SQ-CO_2-MO	SPOC-SQ-a after CO_2 removal
CCDC number	2220262	2220260	2220269
Empirical formula	$C_{28.14394}H_{16}Cl_4N_2O_{2.28788}$	$C_{28}H_{16}Cl_4N_2O_2$	$C_{28}H_{16}Cl_4N_2O_2$
Formula weight	560.56	554.23	554.23
Temperature/K	122(4)	126(12)	120.0(6)
Crystal system	triclinic	triclinic	triclinic
Space group	P-1	P-1	P-1
a/Å	8.725(4)	8.701(6)	12.8242(18)
b/Å	8.867(4)	8.844(12)	13.763(2)
c/Å	9.610(7)	9.591(15)	16.591(3)
α/°	115.92(6)	116.14(15)	110.088(14)
β/°	94.03(5)	93.91(9)	111.009(14)
γ/°	92.15(4)	92.69(9)	91.101(12)
Volume/Å^3	665.1(7)	658.5(15)	2533.2(7)
Z	1	1	4
ρ_{calc}mg/mm^3	1.399	1.398	1.453
m/mm^{-1}	0.475	0.478	0.497
F(000)	285	282	1128
Crystal size/mm^3	0.24 × 0.17 × 0.13	0.12 × 0.11 × 0.09	0.16 × 0.12 × 0.06
2*Θ* range for data collection	6.68 to 51.98°	6.68 to 52°	5.94 to 48°
Index ranges	-10 ≤ h ≤ 9, -10 ≤ k ≤ 10, -11 ≤ l ≤ 11	-10 ≤ h ≤ 9, -10 ≤ k ≤ 8, -9 ≤ l ≤ 11	-14 ≤ h ≤ 14, -14 ≤ k ≤ 15, -17 ≤ l ≤ 18
Reflections collected	4178	3704	15254
Independent reflections	2556[R(int) = 0.1127 (inf-0.9Å)]	2477[R(int) = 0.2016 (inf-0.9Å)]	7919[R(int) = 0.1555 (inf-0.9Å)]
Data/restraints/parameters	2556/13/173	2477/152/139	7919/432/649

Goodness-of-fit on F^2	1.037	0.971	1.017
Final R indexes [$I>=2\sigma(I)$]	R_1 = 0.1178, wR_2 = 0.2284	R_1 = 0.1284, wR_2 = 0.2258	R_1 = 0.1100, wR_2 = 0.1930
Final R indexes [all data]	R_1 = 0.2309, wR_2 = 0.3000	R_1 = 0.4068, wR_2 = 0.3617	R_1 = 0.2652, wR_2 = 0.2679
Largest diff. peak/hole / e Å^{-3}	0.647/-0.389	0.382/-0.336	1.453/-0.349
Flack Parameters	N	N	N
Completeness	0.9916	0.9732	0.9957

$R_1 = \Sigma||F_o| - |F_c||/\Sigma|F_o|$, $wR_2 = [\Sigma w(F_o^2 - F_c^2)^2/\Sigma w(F_o^2)^2]^{1/2}$

Table S3. Crystal data and structure refinement of SPOC-SQ-C_2H_2, SPOC-SQ-C_2H_2-MO, and SPOC-SQ-a after C_2H_2 removal.

Name	SPOC-SQ-C_2H_2	SPOC-SQ-C_2H_2-MO	SPOC-SQ-a after C_2H_2 removal
CCDC number	2034380	2220253	2220252
Empirical formula	$C_{30.10044}H_{18.10044}Cl_4N_2O_2$	$C_{28}H_{16}Cl_4N_2O_2$	$C_{28}H_{16}Cl_4N_2O_2$
Formula weight	581.57	554.23	554.23
Temperature/K	119(5)	113.40(14)	106.0(10)
Crystal system	triclinic	triclinic	triclinic
Space group	P-1	P-1	P-1
a/Å	8.7325(10)	8.690(14)	12.8312(18)
b/Å	8.8710(9)	8.914(13)	13.764(2)
c/Å	9.6585(14)	9.585(17)	16.547(2)
α/°	94.715(10)	116.08(15)	110.050(13)
β/°	115.018(13)	93.95(14)	111.046(13)
γ/°	90.156(9)	92.71(12)	91.168(12)
Volume/Å^3	675.13(14)	662.77(18)	2527.5(6)
Z	1	1	4
ρ_{calc}mg/mm^3	1.430	1.389	1.457
m/mm^{-1}	0.470	0.475	0.498
F(000)	297	282	1128
Crystal size/mm^3	0.34 × 0.32 × 0.23	0.22 × 0.18 × 0.12	0.28 × 0.26 × 0.12
2Θ range for data collection	6.26 to 51.98°	7 to 52°	6.36 to 52°
Index ranges	-10 ≤ h ≤ 10, -10 ≤ k ≤ 9,	-10 ≤ h ≤ 10, -10 ≤ k ≤ 10,	-14 ≤ h ≤ 15, -16 ≤ k ≤ 16,

	-11 ≤ l ≤ 9	-9 ≤ l ≤ 11	-20 ≤ l ≤ 19
Reflections collected	4542	4178	16995
Independent reflections	2639[R(int) = 0.0404 (inf-0.9Å)]	2524[R(int) = 0.0513 (inf-0.9Å)]	9574[R(int) = 0.1439 (inf-0.9Å)]
Data/restraints/parameters	2639/2/183	2524/0/163	9574/584/649
Goodness-of-fit on F^2	1.093	1.045	0.980
Final R indexes [I>=2σ (I)]	R_1 = 0.0597, wR_2 = 0.1288	R_1 = 0.0615, wR_2 = 0.1158	R_1 = 0.1081, wR_2 = 0.1694
Final R indexes [all data]	R_1 = 0.0852, wR_2 = 0.1436	R_1 = 0.1041, wR_2 = 0.1435	R_1 = 0.2633, wR_2 = 0.2414
Largest diff. peak/hole/eÅ^{-3}	0.309/-0.283	0.436/-0.390	1.091/-0.374
Flack Parameters	N	N	N
Completeness	0.9949	0.9873	0.9939

$R_1 = \Sigma||F_o| - |F_c||/\Sigma|F_o|$, $wR_2 = [\Sigma w(F_o^2 - F_c^2)^2/\Sigma w(F_o^2)^2]^{1/2}$

Table S4. Crystal data and structure refinement of SPOC-SQ-C_2H_4, SPOC-SQ-C_2H_4-MO, SPOC-SQ-C_2H_4-MSO, and SPOC-SQ-a after C_2H_4 removal.

Name	SPOC-SQ-C_2H_4	SPOC-SQ-C_2H_4-MO	SPOC-SQ-C_2H_4-MSO	SPOC-SQ-a after C_2H_4 removal
CCDC number	2220258	2220254	2220255	2220265
Empirical formula	$C_{29.10898}H_{18.21796}Cl_4N_2O_2$	$C_{28}H_{16}Cl_4N_2O_2$	$C_{28}H_{16}Cl_4N_2O_2$	$C_{28}H_{16}Cl_4N_2O_2$
Formula weight	569.78	554.23	554.23	554.23
Temperature/K	116(2)	116(3)	114.55(10)	113.3(2)
Crystal system	triclinic	triclinic	triclinic	triclinic
Space group	P-1	P-1	P-1	P-1
a/Å	8.7378(12)	8.733(2)	9.314(11)	12.826(4)
b/Å	8.8280(14)	8.842(2)	9.507(6)	13.793(3)
c/Å	9.6641(17)	9.538(2)	14.399(9)	16.617(4)
α/°	93.944(14)	115.68(2)	87.70(6)	110.09(2)
β/°	115.342(15)	93.96(2)	85.83(8)	111.15(3)
γ/°	91.202(12)	92.18(2)	86.04(7)	90.96(2)
Volume/Å^3	671.08(18)	660.2(3)	1267.8(19)	2541.5(11)
Z	1	1	2	4
ρ_{calc}mg/mm^3	1.410	1.394	1.452	1.448
m/mm^{-1}	0.471	0.477	0.497	0.495

$F(000)$	291	282	564	1128
Crystal size/mm^3	0.34 × 0.23 × 0.11	0.28 × 0.24 × 0.22	0.32 × 0.23 × 0.18	0.35 × 0.34 × 0.27
2Θ range for data collection	6.74 to 51.98°	6.36 to 45.98°	5.94 to 51.98°	6.74 to 52°
Index ranges	-10 ≤ h ≤ 10, -10 ≤ k ≤ 9, -11 ≤ l ≤ 11	-9 ≤ h ≤ 9, -9 ≤ k ≤ 9, -9 ≤ l ≤ 10	-11 ≤ h ≤ 11, -9 ≤ k ≤ 11, -17 ≤ l ≤ 15	-14 ≤ h ≤ 15, -17 ≤ k ≤ 16, -20 ≤ l ≤ 20
Reflections collected	4306	3329	8774	17355
Independent reflections	2613[R(int) = 0.0517 (inf-0.9Å)]	1824[R(int) = 0.0734 (inf-0.9Å)]	4872[R(int) = 0.2131 (inf-0.9Å)]	9766[R(int) = 0.1089 (inf-0.9Å)]
Data/restraints/parameters	2613/7/173	1824/146/163	4872/615/413	9766/420/649
Goodness-of-fit on F^2	1.102	1.095	1.022	1.214
Final R indexes [$I>=2\sigma(I)$]	R_1 = 0.0743, wR_2 = 0.1540	R_1 = 0.0833, wR_2 = 0.2239	R_1 = 0.1735, wR_2 = 0.3428	R_1 = 0.1645, wR_2 = 0.3660
Final R indexes [all data]	R_1 = 0.1116, wR_2 = 0.1803	R_1 = 0.1283, wR_2 = 0.2584	R_1 = 0.4401, wR_2 = 0.5069	R_1 = 0.2598, wR_2 = 0.4550
Largest diff. peak/hole / e Å^{-3}	0.396/-0.494	1.016/-0.341	0.459/-0.403	3.058/-0.623
Flack Parameters	N	N	N	N
Completeness	0.9909	0.9864	0.9905	0.9772

$R_1 = \Sigma||F_o| - |F_c||/\Sigma|F_o|$, $wR_2 = [\Sigma w(F_o^2 - F_c^2)^2/\Sigma w(F_o^2)^2]^{1/2}$

Table S5. Crystal data and structure refinement of SPOC-SQ-C_2H_6, SPOC-SQ-C_2H_6-MO, SPOC-SQ-C_2H_6-MSO, and SPOC-SQ-a after C_2H_6 removal.

Name	SPOC-SQ-C_2H_6	SPOC-SQ-C_2H_6-MO	SPOC-SQ-C_2H_6-MSO	SPOC-SQ-a after C_2H_6 removal
CCDC number	2220268	2220264	2220266	2220267
Empirical formula	$C_{29.85152}H_{21.55456}Cl_4N_2O_2$	$C_{28}H_{16}Cl_4N_2O_2$	$C_{28}H_{16}Cl_4N_2O_2$	$C_{28}H_{16}Cl_4N_2O_2$
Formula weight	582.06	554.23	554.23	554.23
Temperature/K	119(7)	113.20(14)	115(2)	113.45(10)
Crystal system	triclinic	triclinic	triclinic	triclinic
Space group	P-1	P-1	P-1	P-1
a/Å	8.064(3)	8.739(4)	9.287(4)	12.831(3)
b/Å	9.307(3)	8.822(4)	9.482(4)	13.765(3)
c/Å	9.775(4)	9.625(5)	14.333(5)	16.563(4)

α/°	86.73(3)	93.92(4)	87.69(3)	110.06(2)
β/°	68.69(3)	115.31(5)	85.95(3)	111.036(19)
γ/°	86.29(3)	91.50(4)	85.88(3)	91.065(17)
Volume/Å^3	681.5(4)	668.0(5)	1254.9(8)	2531.1(9)
Z	1	1	2	4
ρ_{calc}mg/mm^3	1.418	1.378	1.467	1.454
m/mm^{-1}	0.466	0.471	0.502	0.498
F(000)	299	282	564	1128
Crystal size/mm^3	0.55 × 0.48 × 0.43	0.43 × 0.41 × 0.40	0.23 × 0.22 × 0.21	0.32 × 0.32 × 0.15
2Θ range for data collection	6.82 to 51.98°	6.88 to 51.98°	6.96 to 52°	6.74 to 52°
Index ranges	-7 ≤ h ≤ 9, -10 ≤ k ≤ 11, -12 ≤ l ≤ 11	-9 ≤ h ≤ 10, -10 ≤ k ≤ 10, -11 ≤ l ≤ 11	-11 ≤ h ≤ 11, -7 ≤ k ≤ 11, -15 ≤ l ≤ 17	-15 ≤ h ≤ 15, -16 ≤ k ≤ 16, -18 ≤ l ≤ 20
Reflections collected	4452	4057	6627	17818
Independent reflections	2607[R(int) = 0.1153 (inf-0.9Å)]	2535[R(int) = 0.1245 (inf-0.9Å)]	4637[R(int) = 0.1353 (inf-0.9Å)]	9589[R(int) = 0.1559 (inf-0.9Å)]
Data/restraints/parameters	2607/0/174	2535/102/163	4637/633/401	9589/414/649
Goodness-of-fit on F^2	1.079	1.183	1.011	1.032
Final R indexes [I>=2σ (I)]	R_1 = 0.1385, wR_2 = 0.3236	R_1 = 0.1688, wR_2 = 0.3575	R_1 = 0.1536, wR_2 = 0.3419	R_1 = 0.1373, wR_2 = 0.2836
Final R indexes [all data]	R_1 = 0.2047, wR_2 = 0.3931	R_1 = 0.2819, wR_2 = 0.4323	R_1 = 0.3689, wR_2 = 0.5030	R_1 = 0.3314, wR_2 = 0.4074
Largest diff. peak/hole / e Å^{-3}	1.178/-0.684	0.894/-0.516	0.719/-0.819	1.523/-0.451
Flack Parameters	N	N	N	N
Completeness	0.9719	0.9870	0.9642	0.9865

$R_1 = \Sigma||F_o| - |F_c||/\Sigma|F_o|$, $wR_2 = [\Sigma w(F_o^2 - F_c^2)^2/\Sigma w(F_o^2)^2]^{1/2}$

Table S6. Crystal data and structure refinement of crystals SPOC-SQ-C_3H_4 and SPOC-SQ-a after C_3H_4 removal.

Name	SPOC-SQ-C_3H_4	SPOC-SQ-a after C_3H_4 removal
CCDC number	2220257	2220261
Empirical formula	$C_{31}H_{20}Cl_4N_2O_2$	$C_{28}H_{16}Cl_4N_2O_2$
Formula weight	594.29	554.23
Temperature/K	114(4)	111.55(10)
Crystal system	triclinic	triclinic
Space group	P-1	P-1
a/Å	6.9024(19)	12.870(3)
b/Å	9.767(3)	13.804(4)
c/Å	10.398(3)	16.626(5)
α/°	103.85(2)	109.91(3)
β/°	102.38(2)	111.03(2)
γ/°	91.68(2)	91.26(2)
Volume/Å^3	662.4(3)	2556.9(12)
Z	1	4
ρ_{calc}mg/mm^3	1.490	1.440
m/mm^{-1}	0.481	0.492
F(000)	304	1128
Crystal size/mm^3	0.35 × 0.34 × 0.13	0.31 × 0.23 × 0.22
2*Θ* range for data collection	6.7 to 52°	5.92 to 48°
Index ranges	-7 ≤ h ≤ 8, -11 ≤ k ≤ 12, -12 ≤ l ≤ 11	-14 ≤ h ≤ 12, -15 ≤ k ≤ 15, -13 ≤ l ≤ 19
Reflections collected	4029	12604
Independent reflections	2527[R(int) = 0.0789 (inf-0.9Å)]	7760[R(int) = 0.1713 (inf-0.9Å)]
Data/restraints/parameters	2527/24/191	7760/584/649
Goodness-of-fit on F^2	1.052	1.038
Final *R* indexes [$I>=2\sigma(I)$]	R_1 = 0.1050, wR_2 = 0.2427	R_1 = 0.1389, wR_2 = 0.2944
Final *R* indexes [all data]	R_1 = 0.1665, wR_2 = 0.2975	R_1 = 0.3133, wR_2 = 0.4402
Largest diff. peak/hole / e Å^{-3}	1.013/-0.565	1.091/-0.504
Flack Parameters	N	N
Completeness	0.9836	0.9638

$R_1 = \Sigma||F_o| - |F_c||/\Sigma|F_o|$, $wR_2 = [\Sigma w(F_o^2 - F_c^2)^2/\Sigma w(F_o^2)^2]^{1/2}$

Table S7. Crystal data and structure refinement of crystals SPOC-SQ-C_3H_6, SPOC-SQ-C_3H_6-MO, and SPOC-SQ-a after C_3H_6 removal.

Name	SPOC-SQ-C_3H_6	SPOC-SQ-C_3H_6-MO	SPOC-SQ-a after C_3H_6 removal
CCDC number	2220256	2220263	2220259
Empirical formula	$C_{31}H_{22}Cl_4N_2O_2$	$C_{28}H_{16}Cl_4N_2O_2$	$C_{56}H_{32}Cl_8N_4O_4$
Formula weight	596.31	554.23	1108.46
Temperature/K	121(6)	112.2(14)	118.05(10)
Crystal system	triclinic	triclinic	triclinic
Space group	P-1	P-1	P-1
a/Å	8.530(3)	9.121(11)	12.862(4)
b/Å	9.049(3)	9.918(7)	13.775(4)
c/Å	9.934(3)	15.597(11)	16.600(6)
α/°	94.20(3)	79.67(6)	110.12(3)
β/°	115.28(4)	86.30(8)	111.23(3)
γ/°	91.16(3)	85.92(8)	90.97(3)
Volume/Å^3	690.4(4)	1383(2)	2540.4(14)
Z	1	2	2
ρ_{calc}mg/mm^3	1.434	1.331	1.449
m/mm^{-1}	0.462	0.455	0.496
F(000)	306	564	1128
Crystal size/mm^3	0.14 × 0.14 × 0.13	0.24 × 0.21 × 0.13	0.20 × 0.18 × 0.11
2*Θ* range for data collection	6.76 to 52°	5.94 to 52°	6.34 to 52°
Index ranges	-10 ≤ h ≤ 10, -10 ≤ k ≤ 11, -10 ≤ l ≤ 12	-11 ≤ h ≤ 10, -9 ≤ k ≤ 12, -19 ≤ l ≤ 18	-15 ≤ h ≤ 11, -16 ≤ k ≤ 16, -20 ≤ l ≤ 20
Reflections collected	4202	8460	18986
Independent reflections	2660[R(int) = 0.0689 (inf-0.9Å)]	5210[R(int) = 0.2088 (inf-0.9Å)]	9730[R(int) = 0.1679 (inf-0.9Å)]
Data/restraints/parameters	2660/19/191	5210/334/265	9730/420/649
Goodness-of-fit on F^2	1.096	1.466	1.026
Final *R* indexes [*I*>=2*σ* (*I*)]	R_1 = 0.0981, wR_2 = 0.1784	R_1 = 0.2880, wR_2 = 0.5844	R_1 = 0.1390, wR_2 = 0.3104
Final *R* indexes [all data]	R_1 = 0.1729, wR_2 = 0.2216	R_1 = 0.4898, wR_2 = 0.6500	R_1 = 0.3354, wR_2 = 0.4257
Largest diff. peak/hole/eÅ^{-3}	0.533/-0.342	1.751/-0.755	1.289/-0.487

Flack Parameters	N	N	N
Completeness	0.9770	0.9727	0.9939

$R_1 = \Sigma||F_o| - |F_c||/\Sigma|F_o|$, $wR_2 = [\Sigma w(F_o^2 - F_c^2)^2/\Sigma w(F_o^2)^2]^{1/2}$

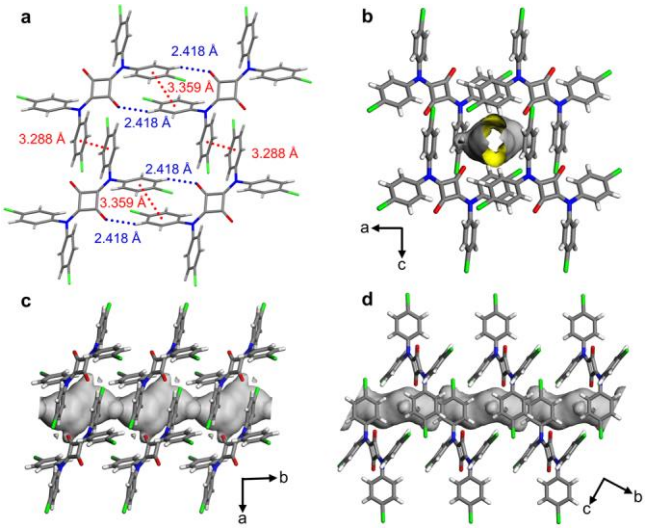

Figure S5. (a) The intermolecular interactions between SPOC-SQ molecules for the framework of SPOC-SQ-CO_2. (b-d) Packing diagrams of SPOC-SQ-CO_2 with the solvent-accessible void space visualized by yellow/grey (inner/outer) curved planes generated with a probe of 1.4 Å. Gray, blue, red, green, and white represent C, N, O, Cl, and H, respectively.

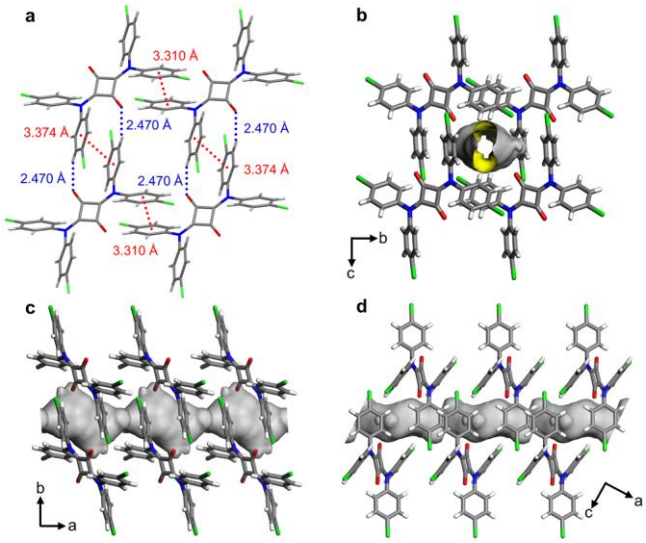

Figure S6. (a) The intermolecular interactions between SPOC-SQ molecules for the framework of SPOC-SQ-C_2H_4. (b-d) Packing diagrams of SPOC-SQ-C_2H_4 with the solvent-accessible void space visualized by yellow/grey (inner/outer) curved planes generated with a probe of 1.4 Å. Gray, blue, red, green, and white represent C, N, O, Cl, and H, respectively.

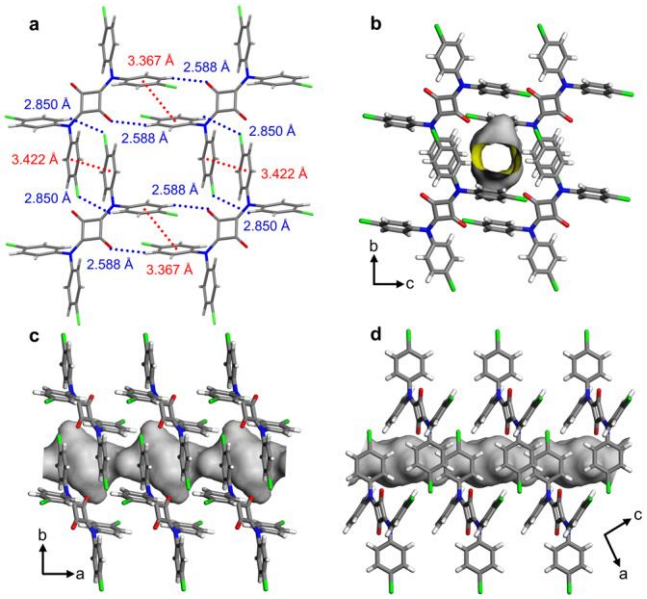

Figure S7. (a) The intermolecular interactions between SPOC-SQ molecules for the framework of SPOC-SQ-C_2H_6. (b-d) packing diagrams of SPOC-SQ-C_2H_6 with the solvent-accessible void space visualized by yellow/grey (inner/outer) curved planes generated with a probe of 1.4 Å. Gray, blue, red, green, and white represent C, N, O, Cl, and H, respectively.

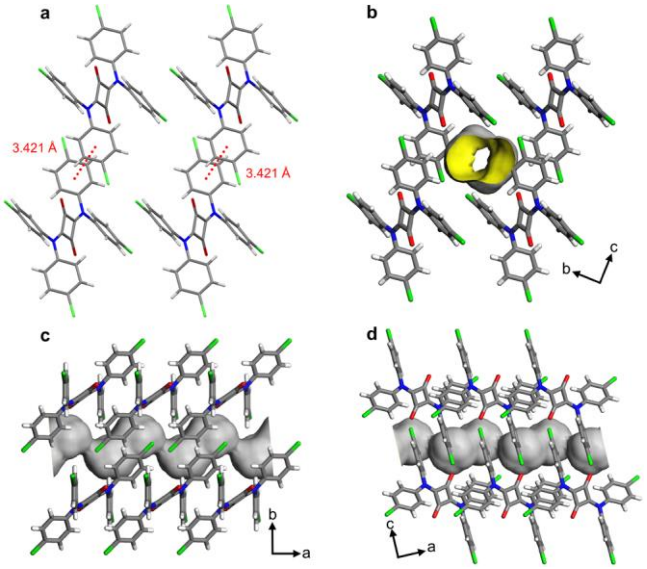

Figure S8. (a) The intermolecular interactions between SPOC-SQ molecules for the framework of SPOC-SQ-C_3H_4. (b-d) Packing diagrams of SPOC-SQ-C_3H_4 with the solvent-accessible void space visualized by yellow/grey (inner/outer) curved planes generated with a probe of 1.4 Å. Gray, blue, red, green, and white represent C, N, O, Cl, and H, respectively.

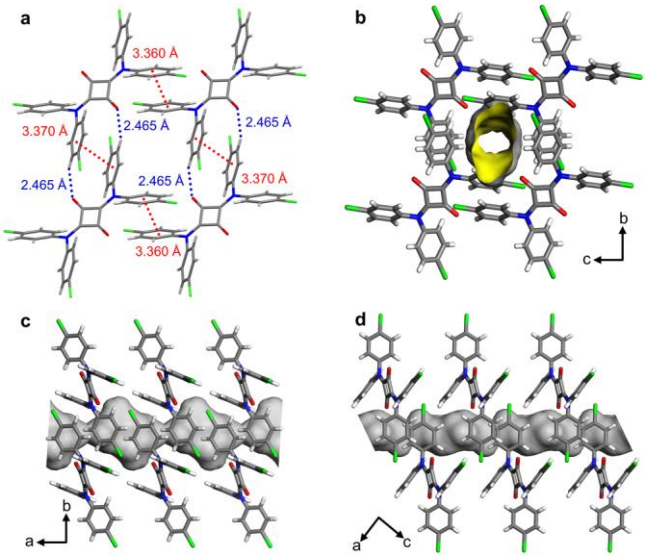

Figure S9. (a) The intermolecular interactions between SPOC-SQ molecules for the framework of SPOC-SQ-C_3H_6. (b-d) Packing diagrams of SPOC-SQ-C_3H_6 with the solvent-accessible void space visualized by yellow/grey (inner/outer) curved planes generated with a probe of 1.4 Å. Gray, blue, red, green, and white represent C, N, O, Cl, and H, respectively.

Table S8. The molecular sizes and kinetic diameters for CO_2, C_2H_2, C_2H_4, C_2H_6, C_3H_4, and C_3H_6.

		Molecular size (Å^3)	Kinetic diameter (Å)
CO_2		3.18 × 3.33 × 5.36	3.3
C_2H_2		3.32 × 3.34 × 5.70	3.3
C_2H_4		3.28 × 4.18 × 4.84	4.2
C_2H_6		3.81 × 4.08 × 4.82	4.4
C_3H_4		4.01 × 4.16 × 6.51	4.2
C_3H_6		4.16 × 4.65 × 6.44	4.7

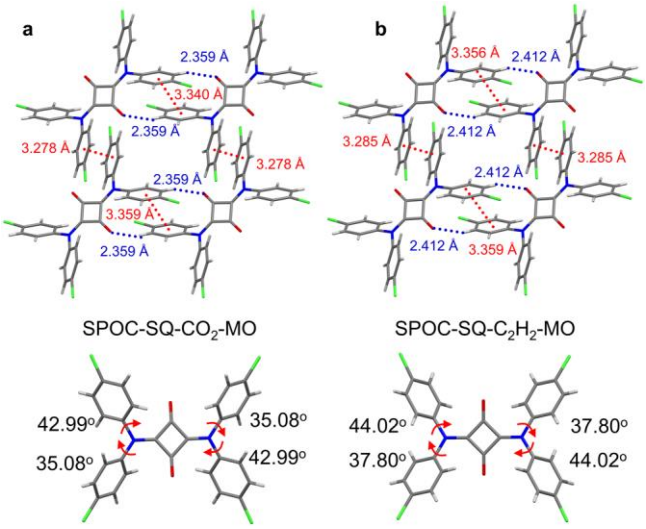

Figure S10. The intermolecular interactions between SPOC-SQ molecules and molecular conformations for the gate-opened frameworks of (a) SPOC-SQ-CO_2-MO and (b) SPOC-SQ-C_2H_2-MO obtained after removal of linear gases. Gray, blue, red, green, and white represent C, N, O, Cl, and H, respectively.

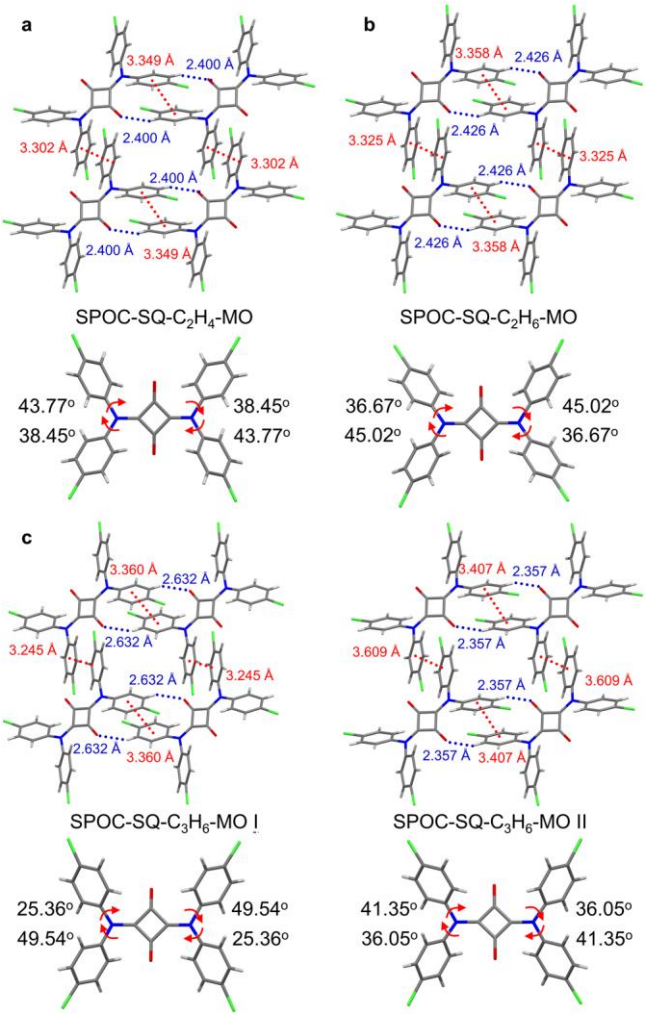

Figure S11. The intermolecular interactions between SPOC-SQ molecules and molecular conformations for the gate-opened frameworks of (a) SPOC-SQ-C_2H_4-MO, (b) SPOC-SQ-C_2H_6-MO, and (c) SPOC-SQ-C_3H_6-MO obtained after removal of nonlinear gases. Among them, there are two kinds of molecular conformations in SPOC-SQ-C_3H_6-MO (I and II) due to the largest disturbance of C_3H_6 to the framework, the average distances of π-π interactions in these two situations were used to analyze. Gray, blue, red, green, and white represent C, N, O, Cl, and H, respectively.

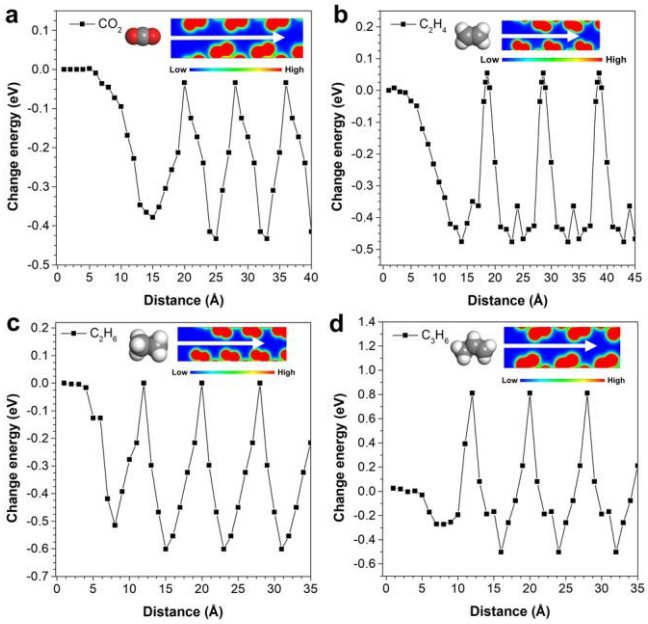

Figure S12. Potential energy profiles of (a) CO_2, (b) C_2H_4, (c) C_2H_6, and (d) C_3H_6 entering SPOC-SQ-gas framework along the central axis of the 1D channel. Insets show the profile of the 1D channel based on the total electron density derived from the DFT calculation. Gray, red, and white represent C, O, and H, respectively.

Table S9. Summary of the maximum and minimum energies and the difference between them upon gas molecules entering 1D channels.

Gas	Max. energy (eV)	Min. energy (eV)	Energy difference value (eV)
CO_2	-0.03418	-0.43245	0.39827
C_2H_4	0.05437	-0.47719	0.53156
C_2H_6	-0.00009	-0.60146	0.60137
C_3H_6	0.81178	-0.50275	1.31453

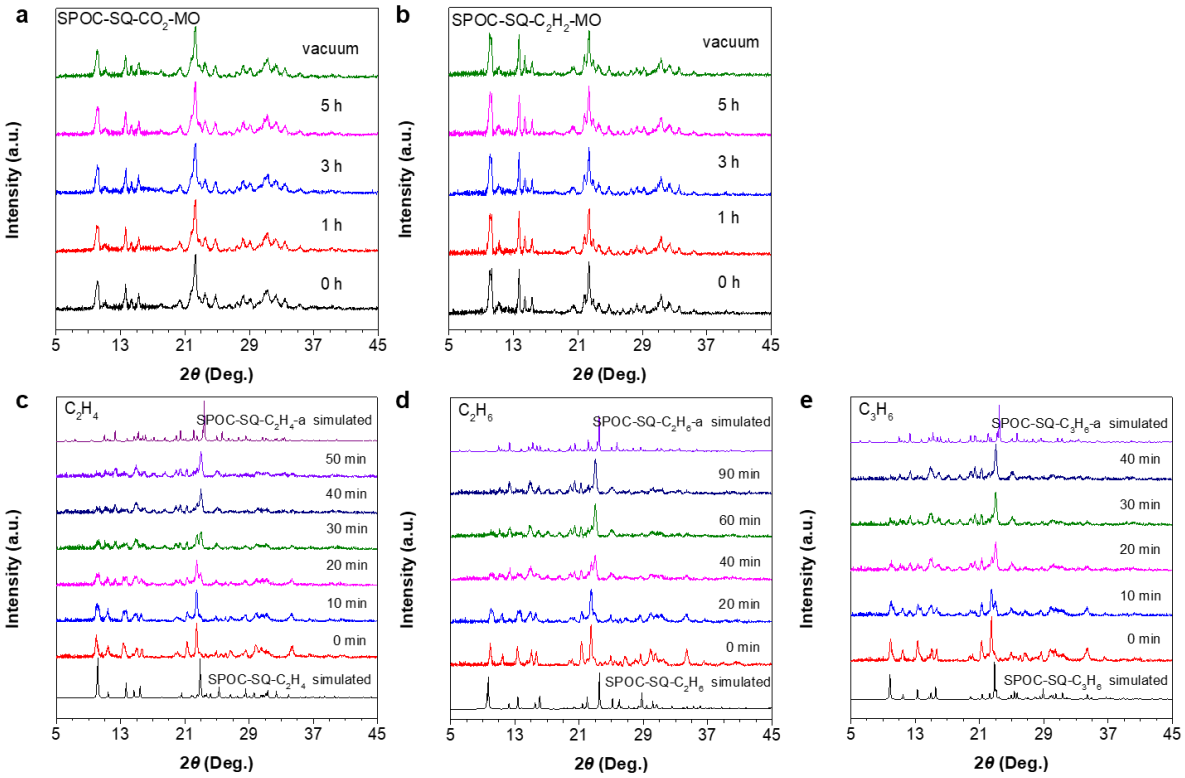

Figure S13. *In-situ* PXRD patterns of (a) SPOC-SQ-CO_2-MO and (b) SPOC-SQ-C_2H_2-MO at room temperature under air or vacuum for different time. *In-situ* PXRD patterns of (c) SPOC-SQ-C_2H_4, (d) SPOC-SQ-C_2H_6, and (e) SPOC-SQ-C_3H_6 single crystals after exposure to room temperature in air for different times, and their simulated PXRD patterns.

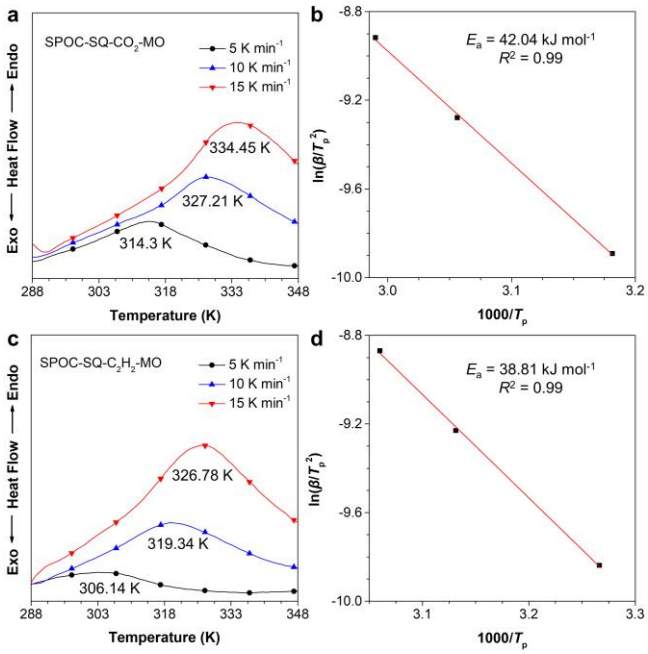

Figure S14. (a and c) DSC traces of (a) SPOC-SQ-CO_2-MO and (c) SPOC-SQ-C_2H_2-MO in the first heating process at heating rates of 5, 10, and 15 K min^{-1}. (b and d) Kissinger plots for the phase transitions of (b) SPOC-SQ-CO_2-MO and (d) SPOC-SQ-C_2H_2-MO. In the Kissinger method, β and T_p denote heating rate and temperature at the maximum of the DSC peak due to the transformation, respectively, and E_a denotes activation energy.

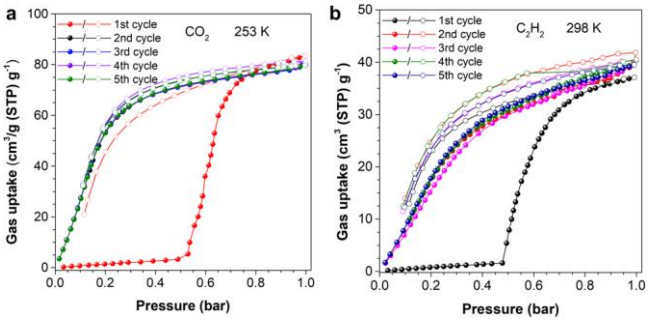

Figure S15. Sorption isotherms of SPOC-SQ-a microcrystals for (a) CO_2 at 253 K and (b) C_2H_2 at 298 K for the first to fifth adsorption-desorption processes. The sample was vacuumed before the second adsorption-desorption processes. Filled and open circle symbols represent adsorption and desorption, respectively.

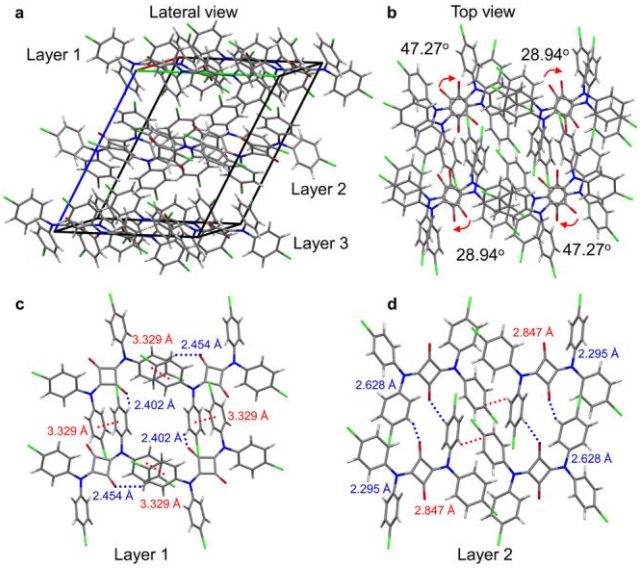

Figure S16. (a) Lateral and (b) top views of the packing diagrams for SPOC-SQ-a after CO_2 removal. (c and d) Intermolecular interactions between SPOC-SQ molecules in (c) layer 1 and (d) layer 2 for SPOC-SQ-a after CO_2 removal. Gray, blue, red, green, and white represent C, N, O, Cl, and H, respectively.

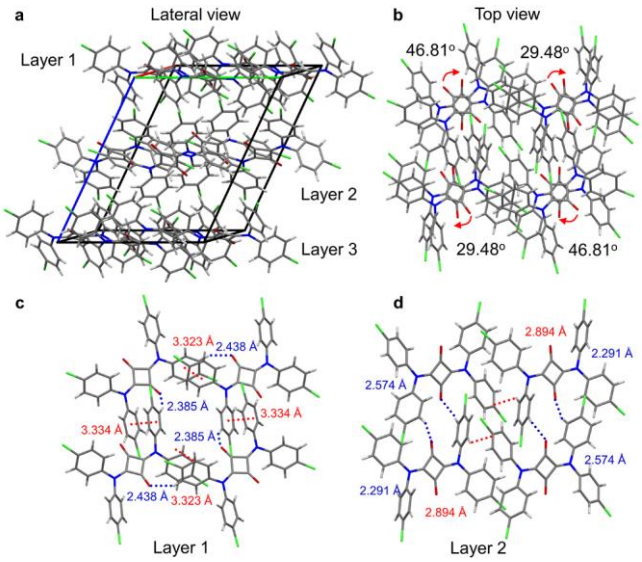

Figure S17. (a) Lateral and (b) top views of the packing diagrams for SPOC-SQ-a after C_2H_2 removal. (c and d) Intermolecular interactions between SPOC-SQ molecules in (c) layer 1 and (d) layer 2 for SPOC-SQ-a after C_2H_2 removal. Gray, blue, red, green, and white represent C, N, O, Cl, and H, respectively.

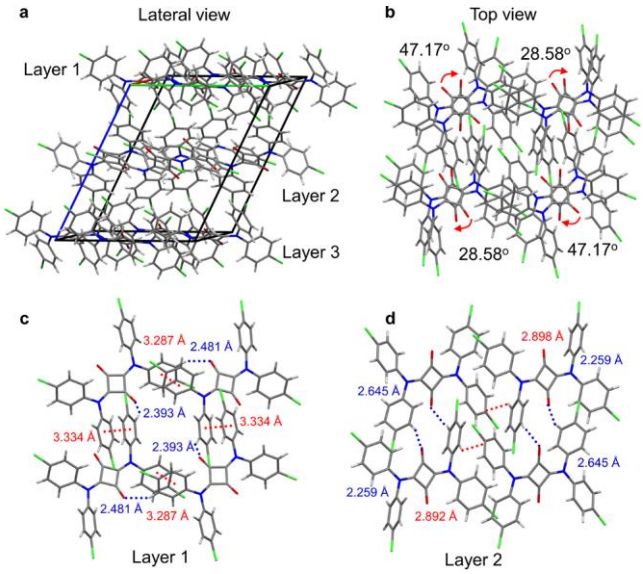

Figure S18. (a) Lateral and (b) top views of the packing diagrams for SPOC-SQ-a after C_2H_4 removal. (c and d) Intermolecular interactions between SPOC-SQ molecules in (c) layer 1 and (d) layer 2 for SPOC-SQ-a after C_2H_4 removal. Gray, blue, red, green, and white represent C, N, O, Cl, and H, respectively.

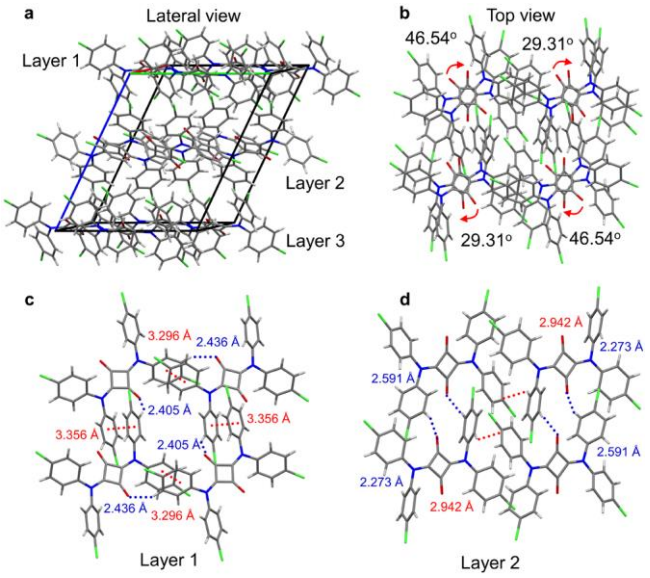

Figure S19. (a) Lateral and (b) top views of the packing diagrams for SPOC-SQ-a after C_2H_6 removal. (c and d) Intermolecular interactions between SPOC-SQ molecules in (c) layer 1 and (d) layer 2 for SPOC-SQ-a after C_2H_6 removal. Gray, blue, red, green, and white represent C, N, O, Cl, and H, respectively.

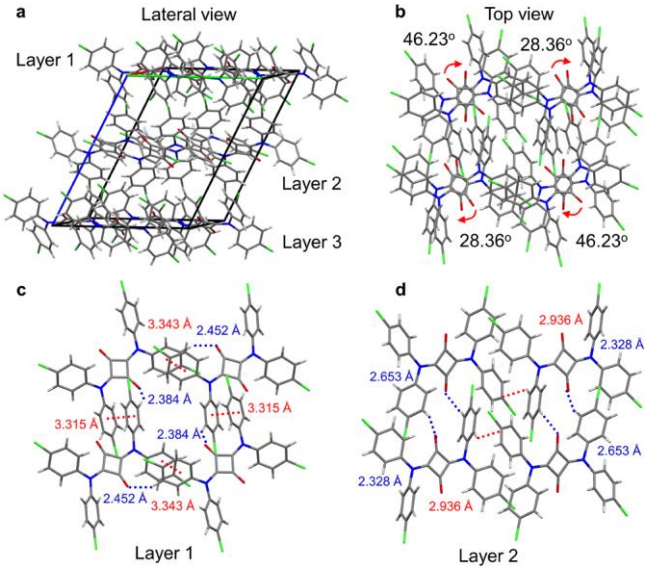

Figure S20. (a) Lateral and (b) top views of the packing diagrams for SPOC-SQ-a after C_3H_6 removal. (c and d) Intermolecular interactions between SPOC-SQ molecules in (c) layer 1 and (d) layer 2 for SPOC-SQ-a after C_3H_6 removal. Gray, blue, red, green, and white represent C, N, O, Cl, and H, respectively.

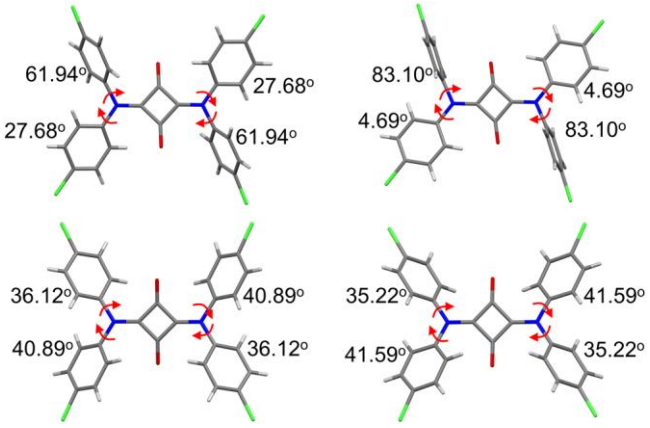

Figure S21. Molecular conformations of SPOC-SQ molecules in SPOC-SQ-a after CO_2 removal. Gray, blue, red, green, and white represent C, N, O, Cl, and H, respectively.

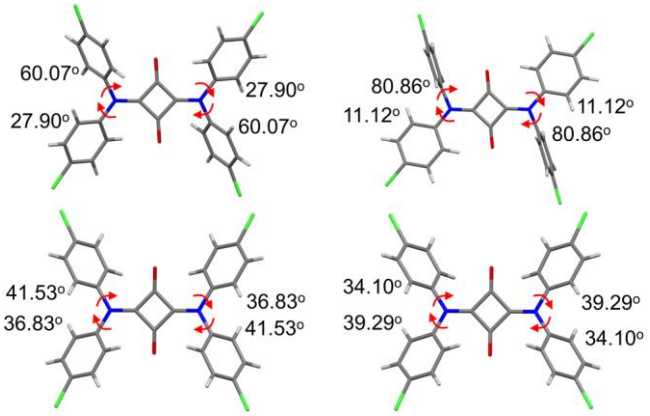

Figure S22. Molecular conformations of SPOC-SQ molecules in SPOC-SQ-a after C_2H_2 removal. Gray, blue, red, green, and white represent C, N, O, Cl, and H, respectively.

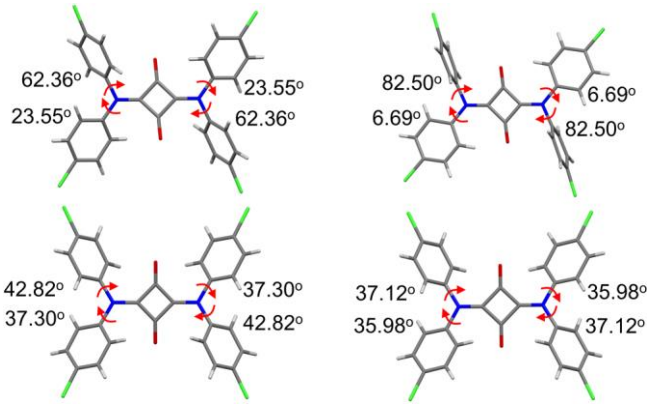

Figure S23. Molecular conformations of SPOC-SQ molecules in SPOC-SQ-a after C_2H_4 removal. Gray, blue, red, green, and white represent C, N, O, Cl, and H, respectively.

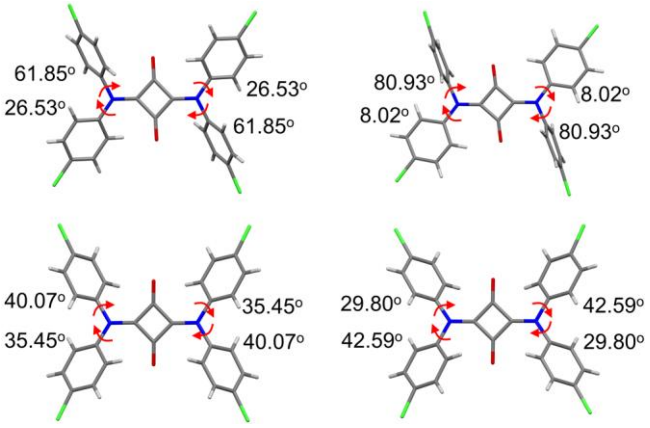

Figure S24. Molecular conformations of SPOC-SQ molecules in SPOC-SQ-a after C_2H_6 removal. Gray, blue, red, green, and white represent C, N, O, Cl, and H, respectively.

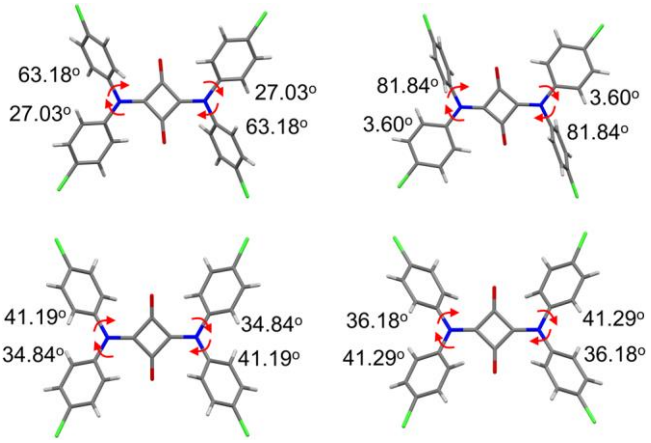

Figure S25. Molecular conformations of SPOC-SQ molecules in SPOC-SQ-a after C_3H_6 removal. Gray, blue, red, green, and white represent C, N, O, Cl, and H, respectively.

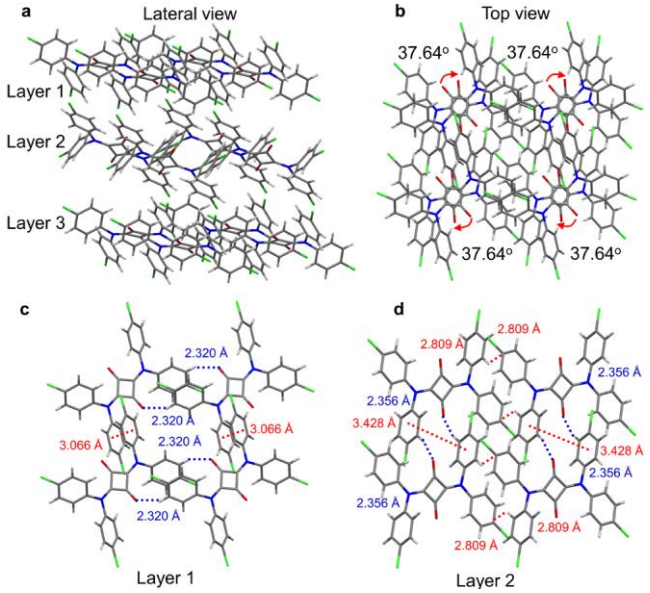

Figure S26. (a) Lateral and (b) top views of the packing diagrams for SPOC-SQ-C_2H_4-MSO after C_2H_4 removal. (c and d) Intermolecular interactions between SPOC-SQ molecules in (c)

layer 1 and (d) layer 2 for SPOC-SQ-C_2H_4-MSO after C_2H_4 removal. Gray, blue, red, green, and white represent C, N, O, Cl, and H, respectively.

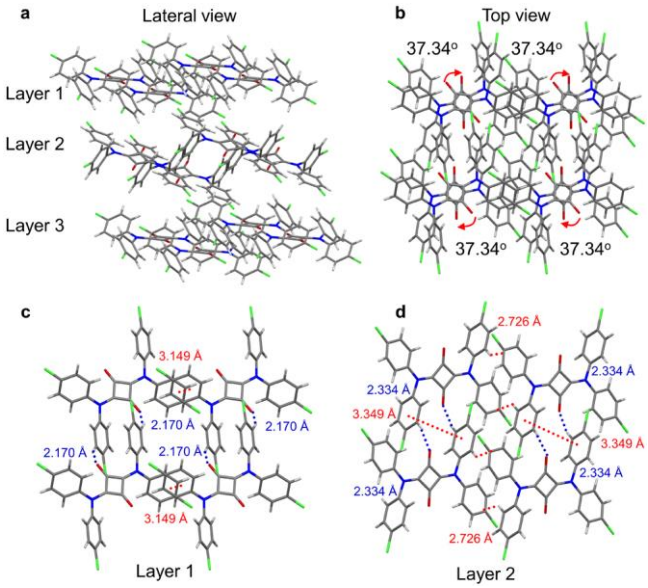

Figure S27. (a) Lateral and (b) top views of the packing diagrams for SPOC-SQ-C_2H_6-MSO after C_2H_6 removal. (c and d) Intermolecular interactions between SPOC-SQ molecules in (c) layer 1 and (d) layer 2 for SPOC-SQ-C_2H_6-MSO after C_2H_6 removal. Gray, blue, red, green, and white represent C, N, O, Cl, and H, respectively.

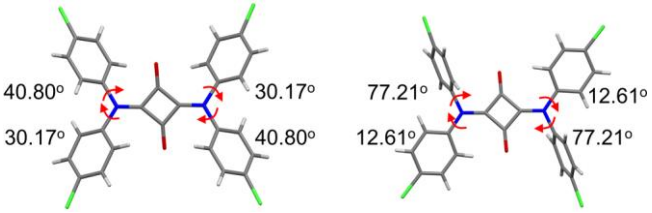

Figure S28. Molecular conformations of SPOC-SQ molecules in SPOC-SQ-C_2H_4-MSO after C_2H_4 removal. Gray, blue, red, green, and white represent C, N, O, Cl, and H, respectively.

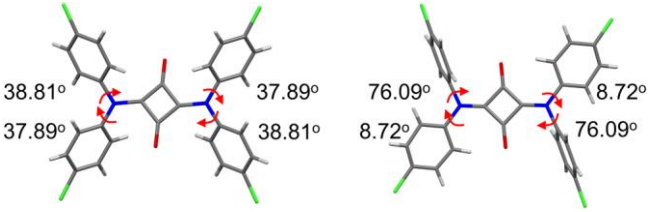

Figure S29. Molecular conformations of SPOC-SQ molecules in SPOC-SQ-C_2H_6-MSO after C_2H_6 removal. Gray, blue, red, green, and white represent C, N, O, Cl, and H, respectively.

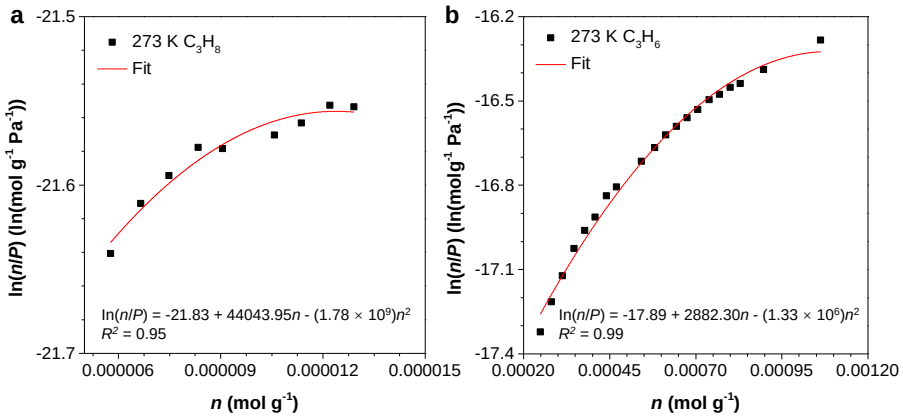

Figure S30. The virial graphs for adsorption of (a) C_3H_8 and (b) C_3H_6 on SPOC-SQ-a crystals at 273 K.

Table S10. Summary of virial parameters (A_0: adsorbate-adsorbent interactions; A_1: adsorbate-adsorbate interactions; R^2: variance; K_H: Henry's law constant), selectivity of gas sorption ($S_{i/C3H8}$: selectivity of C_3H_6 over C_3H_8) on SPOC-SQ-a at 273 K obtained from the virial equation.

Gas	T (K)	A_0 (ln(molg^{-1}Pa^{-1}))	A_1 (g mol^{-1})	A_2 (g mol^{-1})	R^2	K_H	$S_{i/C3H8}$
C_3H_6	273	-17.89 ± 0.044	2883.30 ± 151.30	1.32×10^6 ± 121028.12	0.99	1.69×10^{-8}	51.16
C_3H_8	273	-21.83 ± 0.04	44043.95 ± 9082.95	1.78×10^9 ± 4.81×10^8	0.95	3.31×10^{-10}	1

References

[1] J. VandeVondele, M. Krack, F. Mohamed, M. Parrinello, T. Chassaing, J. Hutter, *Comput. Phys. Commun.* **2005**, *167*, 103-128.

[2] S. Goedecker, M. Teter, J. Hutter, *Phys. Rev. B* **1996**, *54*, 1703-1710.

[3] M. Krack, *Chem. Acc.* **2005**, *114*, 145-152.

[4] J. VandeVondele, J. Hutter, *J. Chem. Phys.* **2007**, *127*, 114105.

[5] J. SMoellmann, S. Grimme, *J. Phys. Chem. C* **2014**, *118*, 7615-7621.